PROCEEDINGS OF SPIE

A comparison between the opto-thermo-mechanical model and lab measurements for CHEOPS

Magrin, Demetrio, Viotto, Valentina, Beck, Thomas, Bruno, Giordano, Baroni, Marco, et al.

SPIE.

A comparison between the opto-thermo-mechanical model and lab measurements for CHEOPS

Demetrio Magrin[a], Valentina Viotto[a], Thomas Beck[b], Giordano Bruno[b], Marco Baroni[c], Andrea Turella[c], Massimo Marinai[c], Maria Bergomi[a], Federico Biondi[a], Matteo Munari[d], Luca Marafatto[a], Jacopo Farinato[a], Davide Greggio[a], Marco Dima[a], Gaetano Scandariato[d], Isabella Pagano[d], Roberto Ragazzoni[a], Martin Rieder[b], Martin Diego Busch[b], Daniele Piazza[b], Timothy Bandy[b], Christopher Broeg[b], Andrea Fortier[b], Eduardo Hernandez[b], Virginie Cessa[b], Willy Benz[b], Giampaolo Piotto[e], Ester Giannuzzo[c], Michele Dami[c], Enrico Battistelli[c], Mario Salatti[f], Elisabetta Tommasi[f], Luigi De Angelis[f], Atul Deep[g], Ivan Ngan[g], Francesco Ratti[g], Lisa Gambicorti[g], Nicola Rando[g].

[a]INAF – Osservatorio Astronomico di Padova, Vicolo dell'Osservatorio 5, 35122 Padova, Italy
[b]Physics Institute, Space Research & Planetary Sciences, University of Bern, Sidlerstr. 5, CH-3012 Bern, Switzerland
[c]LEONARDO Company - Via delle Officine Galileo, 150013 Campi Bisenzio (FI), Italy
[d]INAF – Osservatorio Astrofisico di Catania, Via S.Sofia 78, 95123 Catania, Italy
[e]Dipartimento di Fisica ed Astronomia – Università degli Studi di Padova, Vicolo dell'Osservatorio 3, 35122 Padova, Italy
[f]ASI - Via del Politecnico, 00133 Roma, Italy
[g]ESA – ESTEC Keplerlaan 1, 2201 AZ Noordwijk, Netherlands

ABSTRACT

CHEOPS is the first small class mission adopted by ESA in the framework of the Cosmic Vision 2015-2025. Its launch is foreseen in early 2019. CHEOPS aims to get transits follow-up measurements of already known exo-planets, hosted by near bright stars (V<12). Thanks to its ultra-high precision photometry, CHEOPS science goal is accurately measure the radii of planets in the super-Earth to Neptune mass range (1<Mplanet/MEarth<20). The knowledge of the radius by transit measurements, combined with the determination of planet mass through radial velocity techniques, will allow the determination/refinement of the bulk density for a large number of small planets during the scheduled 3.5 years life mission. The instrument is mainly composed of a 320 mm aperture diameter Ritchey-Chretien telescope and a Back End Optics, delivering a de-focused star image onto the focal plane. In this paper we describe the opto-thermo-mechanical model of the instrument and the measurements obtained during the opto-mechanical integration and alignment phase at Leonardo company premises, highlighting the level of congruence between the predictions and measurements.

Keywords: CHEOPS, Exoplanets, transits, ESA small mission, optical-thermo-mechanical model, performance verification

1. INTRODUCTION

CHEOPS (CHaracterizing ExOPlanets Satellite) [1, 2, 3, 4, 5] is the first small class mission adopted by ESA in 2014 in the framework of the Cosmic Vision 2015-2025. Its launch is foreseen in early 2019. The mission is dedicated to the characterization and study of already discovered exoplanets orbiting around bright stars (V<12). These scientific goals will be achieved through ultra-high precision photometric observation of planets transits, which mass is already been estimated by mean of ground based radial velocity spectroscopy. The achievable precision is below 20ppm in 6 hours integration time for a G5 star with V-band magnitudes in the range between 6 and 9 mag. The CHEOPS Consortium is led by Switzerland (University of Bern) and includes institutes, agencies and companies from several European countries (Austria, Belgium, France, Germany, Hungary, Italy, Portugal, Spain, Sweden, and the United Kingdom).

A layout of the CHEOPS instrument and the main specifications are shown in Figure 1. The optical configuration is made of a Ritchey-Chretien telescope, which feeds a second optical train named Back End Optics (BEO). The latter is made of a first refractive doublet that collimates the input beam and forms an image of the entrance pupil, where a mask is placed for straylight rejection purposes. The possibility to introduce a diffuser in this location, in order to homogenize the light, was studied in the past but was not implemented [6]. A flat folding mirror bends the beam toward a second refractive doublet that reimages the focal plane at the required plate scale. An e2v CCD47-20, mounted on the Focal Plane Module (FPM), is placed at a certain distance after the optical focal plane in order to obtain a relatively wide defocused PSF. The size of the PSF is the result of a trade-off study between the noise in the stellar image and the straylight signal. The optimal size has been estimated to be the one delivered by a PSF having the 90% encircled energy in 12 pixels radius.

The on-orbit optical focal plane position with respect to the detector is crucial for the size of the PSF. A certain degree of compensation has been introduced by the possibility to actively stabilize the temperature of the telescope tube, i.e. the inter-distance between the primary and secondary mirror (the leverage factor on the focal plane displacement is 50). Given the fact that the compensation range is limited, a model able to describe the focal plane displacement behavior in the different environmental conditions has been developed. The model has been refined with the measured data during the alignment and performance test campaigns.
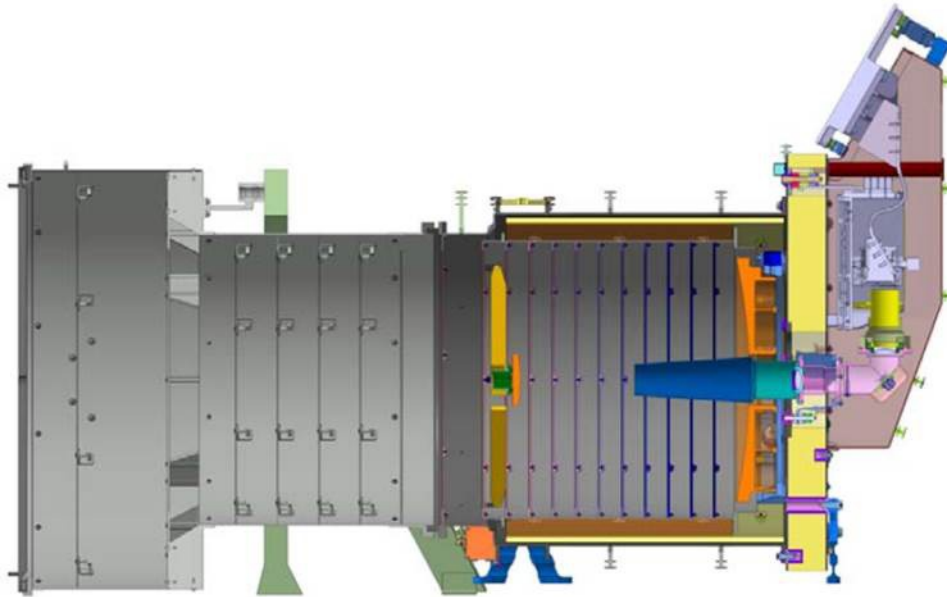
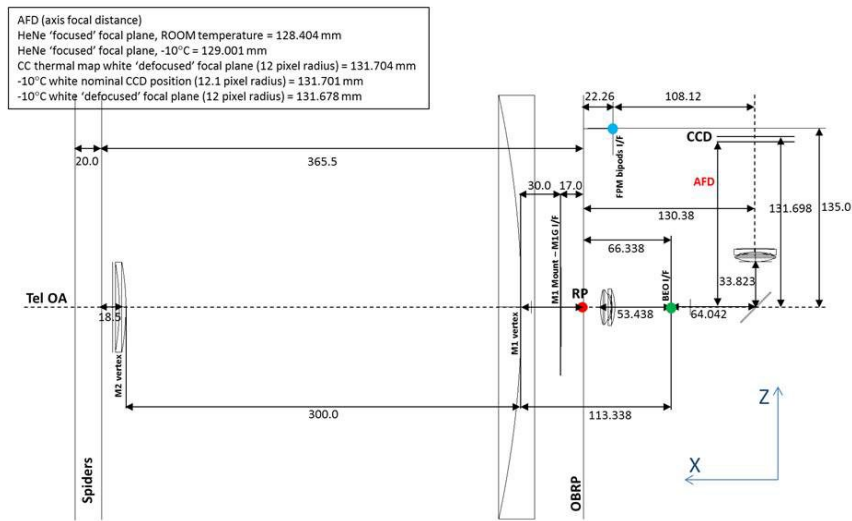| CHEOPS Instrument System	
Entrance pupil diameter	320mm
Central obstruction diameter	68mm
Working F/#	8.38 @ 750 nm
Effective focal length	2681 mm @ 750 nm
Telescope field of view diameter	0.32°
Spectral range	400 – 1100 nm
Pixel size	13 microns
Plate scale	1 arcsec/pixel
Detector focal plane	1024x1024 pixels
Detector Temperature	233K
Detector Stability	10mK
Instrument total Mass	<60kg including system margin
Instrument total nominal power	<60W orbit averaged including margin

Figure 1. A layout of the CHEOPS instrument (Up) and the main specifications (Bottom).

2. THE MODEL

The CHEOPS subsystem aligned and tested during the campaign carried out at the Leonardo company premises is called TEL. It includes the opto-mechanical tube, the primary mirror (M1) and its mount, the secondary mirror (M2), the optical bench assembly, the BEO mechanical housing and the BEO optical elements (D1, M3, D2). The behavior of the TEL subsystem, including the FPM (not part of TEL), as function of the temperature maps, pressure and gravity conditions has been implemented in a mathematical model.

A scheme of the model at room temperature, atmospheric pressure equal to 1 atm and with gravity 1g (with direction and versus equal to x axis) is shows in Figure 2. The reference system introduced in the model, but also utilized during the assembly and alignment phase, is the center of the Optical Bench Reference Plane (red dot in the figure).

Seven thermal maps, used as references, have been implemented in the model. One at room temperature (20°C, 1 atm, 1g along x axis) corresponding to alignment phase environment, three in cryogenic chamber environment (-5°C, -10°C, -15°C, 0 atm, 1g along z axis) corresponding to the performance test campaign conditions and the last three representing the expected hot and cold on orbit temperature distributions. The thermal maps are reported in Figure 3.

Figure 2. Scheme of the model at Room Temperature.

|	Cryogenic Chamber -10°C			Cryogenic Chamber -5°C			Cryogenic Chamber -15°C			Orbit Cold Case Map			Orbit Hot Case Map 1			Orbit Hot Case Map 2		
	T start [°C]	T end [°C]	ΔT [°C]	T start [°C]	T end [°C]	ΔT [°C]	T start [°C]	T end [°C]	ΔT [°C]	T start [°C]	T end [°C]	ΔT [°C]	T start [°C]	T end [°C]	ΔT [°C]	T start [°C]	T end [°C]	ΔT [°C]
M1 mirror	20,000	-10,000	30,000	20,000	-5,000	25,000	20,000	-15,000	35,000	20,000	-16,586	36,586	20,000	-12,586	32,586	20,000	-12,555	32,555
Optical Bench M1 side	20,000	-10,000	30,000	20,000	-5,000	25,000	20,000	-15,000	35,000	20,000	-19,164	39,164	20,000	-13,603	33,603	20,000	-13,125	33,125
FEE legs	20,000	-10,000	30,000	20,000	-5,000	25,000	20,000	-15,000	35,000	20,000	-11,008	31,008	20,000	-7,409	27,409	20,000	-7,226	27,226
BEO housing	20,000	-10,000	30,000	20,000	-5,000	25,000	20,000	-15,000	35,000	20,000	-16,203	36,203	20,000	-13,305	33,305	20,000	-12,636	32,636
Telescope Tube	20,000	-10,000	30,000	20,000	-5,000	25,000	20,000	-15,000	35,000	20,000	-10,618	30,618	20,000	-10,392	30,392	20,000	-10,110	30,110
M2 Assembly	20,000	-10,000	30,000	20,000	-5,000	25,000	20,000	-15,000	35,000	20,000	-29,188	49,188	20,000	-21,300	41,300	20,000	-21,261	41,261
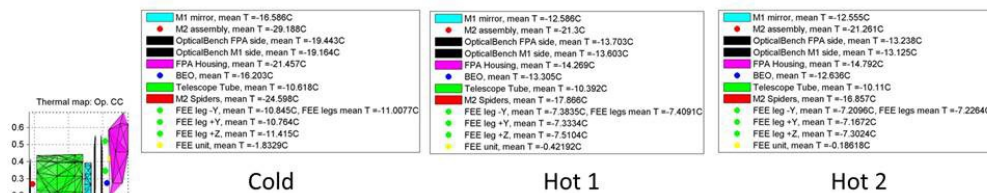
Figure 3. Reference Thermal maps implemented in the model.

The thermal behavior of each component has been estimated independently by analysis. In particular it has been provided by Almatech company for the mechanical parts, by Leonardo company for the optics and by DLR for the FPM. The thermal behavior results have been implemented in the model by computing an equivalent CTE, for each considered element, gauging on the thermal drop between the nominal system configuration (temperature -20C and pressure 1 atm) and the reference working temperature configuration data (Cold orbit, 0 atm for Alamatech data; -10°C, 0 atm for Leonardo data; -27.5°C, 0 atm for DLR). The equivalent CTEs (linear dependency) have been implemented to describe the relative displacements of the following components: M1 mounts to reference point, M1 to M1 mounts, M2 mounts to reference point, M2 to M2 mounts, BEO interface to reference point, D1 to D1 BEO housing interface, M3 to M3 BEO housing interface, D2 to D2 BEO housing interface, D1 BEO housing interface to BEO interface, M3 BEO housing interface to BEO interface, D2 BEO housing interface to BEO interface, pupil mask to BEO interface, FPM interface to reference point and FPM CCD to FPM interface. For refractive elements, the model considers also refractive index dependency by the temperature and pressure. The mounts effects on M1 and M2 shape as function of the temperature have been evaluated and implemented in the model as defocus and trefoil Zernike polynomials.

Both the optical bench and the telescope mechanical tube are made in carbon fiber. In both cryogenic vacuum chamber and orbit environments carbon fiber structures is expected to shrink because of moisture release. Moisture release effect has been estimated by analysis and implemented in the model. In particular, it affects the M1 position, the M2 position, the BEO interface position, and the FPM interface position.
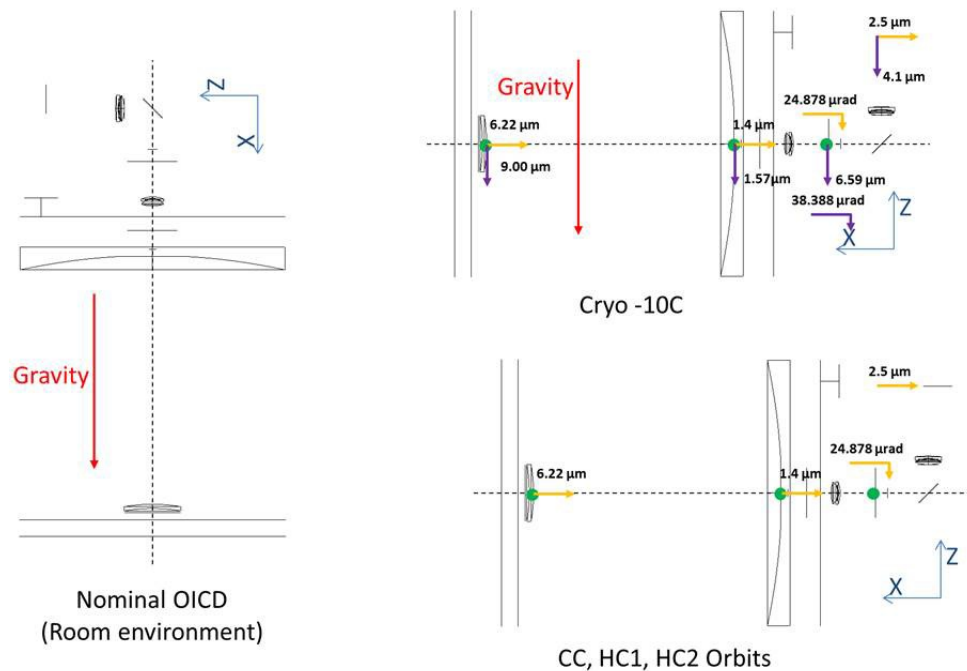

Figure 4. The three configurations considered in the model for gravity effects. TEL in vertical position in room environment with gravity vector pointing from the primary to secondary mirror (left), TEL in vertical position in cryogenic chamber environment with gravity vector pointing from BEO focal plane toward BEO fold mirror (top right) and TEL in orbit (bottom right).

Also 1g-0g gravity-release affects the relative position of the elements. Its effect has been evaluated by analysis and implemented in the model. In particular three configurations have been considered: the telescope in vertical position in room environment with gravity vector pointing from M1 to M2, the telescope in horizontal position in cryogenic chamber environment with gravity vector pointing from BEO focal plane toward M3 and the telescope in orbit (0g assumed). A scheme representing the three configurations and the elements displacement caused by the gravity is shown in Figure 4.

The model has been used also to estimate the expected on orbit performances in terms of delivered size and shape of the PSF by implementing the optics manufacturing and alignment tolerances and the mechanical interfaces settling effects,

due to launch vibrations by mean of a Montecarlo simulation. The description of this analysis is behind the scope of this paper.

The model has been used to describe the behavior of the optical focal plane displacement at TEL level. Never the less, the model can also predict the position of the "defocused" focal plane with respect to the telescope axis, here named Axis Focal Distance (AFD). In particular AFD has been optimized to deliver the best "defocused" PSF in the cold orbit case (PSF having the 90% encircled energy over a radius of 12 pixels). In order to characterize the AFD for each configuration, we have simulated a set of PSFs and computed the encircled energy. Examples of simulated PSFs are shown in Figure 5. They represent the PSFs on the nominal "defocused" focal plane in the configuration with the telescope in vertical position in room environment illuminated with HeNe source, with the telescope in horizontal position in cryogenic environment (-10°C) illuminated with white light source and with the telescope in the cold case orbit illuminated with white light source. In the last case the 90% encircled energy is contained in a circle having radius 12 pixels.
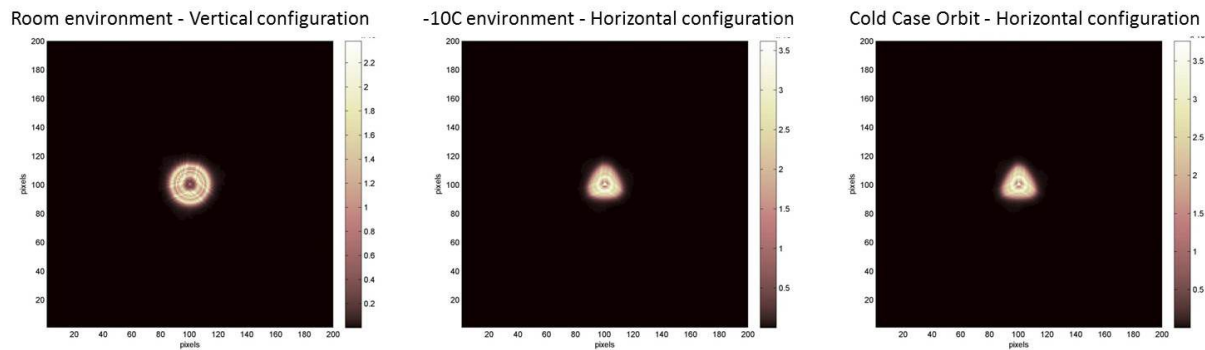

Figure 5. PSFs on the nominal "defocused" focal plane in the configuration with the telescope in vertical position in room environment illuminated with HeNe source (Left), with the telescope in horizontal position in cryogenic environment (-10°C) illuminated with white light source (Center) and with the telescope in the cold case orbit illuminated with white light source (Right).

3. MEASURMENTS CAMPAIGN

The alignment phase of TEL has started in INAF by testing the procedures and the GSE on a prototype [7] and then it has been concluded in Leonardo where the TEL flight model has been assembled, aligned and tested. In the last phase of the alignment campaign the HeNe nominal focal plane in room environment with the telescope in vertical position has been identified by means of the center of curvature of a spherical mirror, used as reference (Figure 6). Previously, both the FPM interface, used as interface for the spherical mirror mounting, on the TEL optical bench and the spherical mirror have been properly characterized through laser tracker measurement. The TEL has been then illuminated in double-pass with a Zygo interferometer and the D2 has been shimmed in order to reach the fringe minimization. For what concerns the focal plane position, the obtained TEL configuration has been assumed to correspond to the model in room environment with telescope in vertical position.
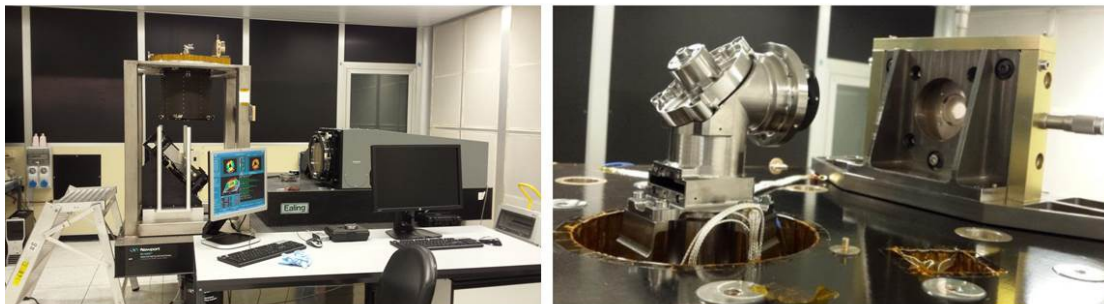

Figure 6. TEL in vertical position illuminated by the interferometer in double pass (Left). The reference spherical mirror mounted on the top of the optical bench (Right).

In the second step the telescope has been placed in horizontal position and illuminated in double-pass with the Zygo interferometer (Figure 7). The measured focal plane relative displacement in room environment from the vertical to the

horizontal configuration was 272 μm. This value is in good accordance with the one predicted by the model, 259 μm, with a discrepancy of only 13 μm. Indeed, given the optical system F/#=8.38, the discrepancy on the focal plane displacement between the measured data and the model translates into a difference on the PSF size of about 0.12 pixels.

In the third step the TEL has been placed in the thermal vacuum chamber in horizontal position for the performance test campaign. A properly designed OGSE (Figure 8), mounted over an hexapod for fine pointing, that allowed the TEL illumination with both FISBA interferometer and white source has been aligned to the telescope, taking advantage again of the illumination in double-pass exploiting the reference spherical mirror.
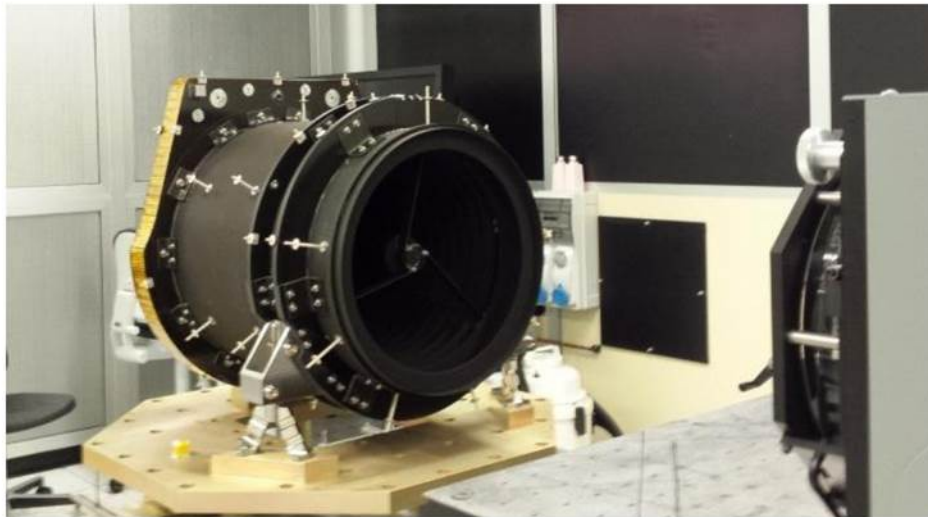

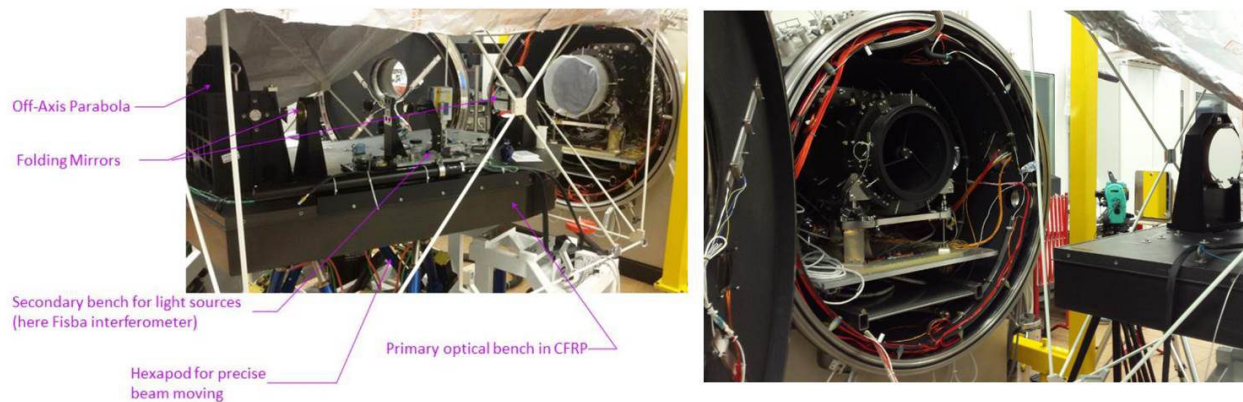Figure 7. TEL in horizontal position in front of the Zygo interferometer.

Figure 8. TEL in horizontal position in front of the OGSE (Left). TEL into the thermal vacuum chamber (Right).

Before starting the thermal-vacuum measurement phase, the reference spherical mirror has been removed and a service detector mounted on a hexapod mechanically decoupled by TEL was mounted instead (Figure 9). The detector position with respect to the focal plane was firstly mechanically characterized with laser tracker equipment and then the position was optically refined by placing it in the best focus of TEL when illuminated by the HeNe source.

A first measurement has been taken in vacuum (10^{-3} Pa) at room temperature (20°C) with the telescope in horizontal configuration with HeNe source. The measured focal plane relative displacement was -95 μm. The model predicted displacement was -77 μm. Also in this case the discrepancy is very small: -18 μm (0.17 pixels on PSF size).

In the last phase the thermal vacuum chamber has been turned on, bringing the TEL to the testing temperatures of -10°C, -15°C and -5°C. At -10°C the measured focal plane relative displacement with HeNe source is -11 μm. The prediction of the model was 417 μm, resulting in a large discrepancy: 428 μm (about 4 pixels on PSF size). It was clear that the thermal behavior was not well described by the model. Even at -15°C and -5°C, we experienced negligible displacements, -14 μm and -4 μm respectively. The focal plane position displacement is much more insensitive to temperature variation than what we expected. In particular the inter-distance between M1 and M2, being the worst offender for the focal plane displacement with a leverage factor of 50, was not well described by the model. We have then corrected its behavior in the model mimicking the measured data.
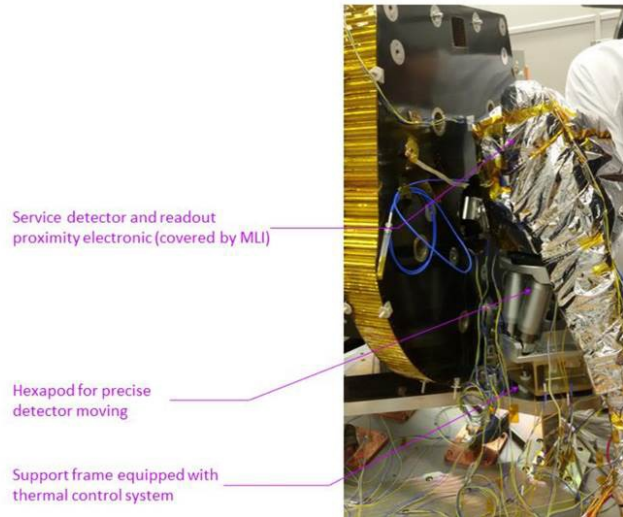

Figure 9. Service detector mounted on the hexapod.

The performance campaign proceeded with the full characterization of the PSFs size and shape over the full Field of View in the "defocused" focal plane at different temperatures. Its description is behind the scope of this paper.

However, the model, after the temperature behavior correction, introducing also the manufacturing and alignment tolerances, was able to deliver synthetic PSFs similar to measured ones in terms of shape and size. An example is shown in Figure 10 where measured and simulated PSFs for the central field with white light illumination in thermal vacuum environment (-10°C) are shown.
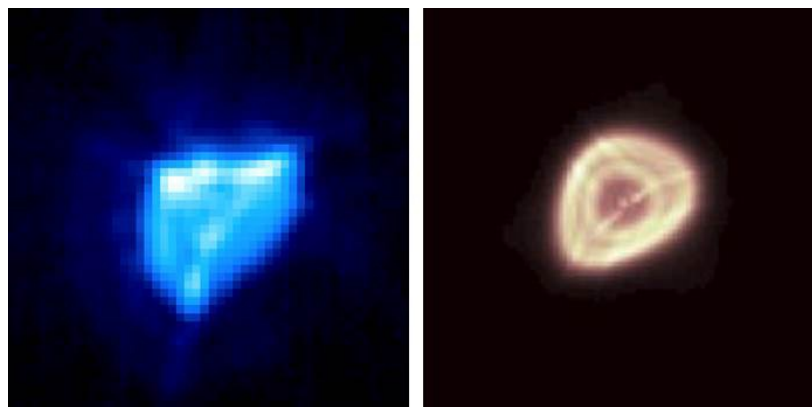

Figure 10. White light measured on axis PSF at -10°C (Left). Simulated white light PSF at -10°C (Right).

4. CONCLUSIONS

CHEOPS is the first small mission in the ESA Science Program. The scientific goal is the study and the characterization of the exoplanets with transits technique by mean of ultra-precise photometric aperture measurements. The CHEOPS performance is directly connected to the PSF size and then to the variation of the optical focal plane with respect to the detector plane. We have developed a mathematical model able to describe and predict the optical focal plane displacement as function of different environmental conditions and in particular the CHEOPS orbital environments. The model has been tested during the TEL alignment and performance campaign. The measured data has been used to improve the model representativeness.

REFERENCES

[1] "CHEOPS − Characterising ExOPlanet Satellite Definition Study Report", ESA/SRE(2013)7, November (2013).

[2] Beck, T., Broeg, C., Fortier, A., Cessa, V., Malvasio, L., Piazza, D., Benz, W., Thomas, N., Magrin, D., Viotto, V., Bergomi, M, Ragazzoni, R., Pagano, I., Peter, G., Buder, M., Plesseria, J. Y., Steller, M.., Ottensamer, R., Ehrenreich, D., Van Damme, C., Isaak, K., Ratti, F., Rando, N., Ngan, I., "CHEOPS: status summary of the instrument development," Proc. SPIE 9904, (2016).

[3] Rando, N., Asquier, J., Corral Van Damme, C., Isaak, K., Ratti, F., Safa, F., Southworth, R., Broeg, C., Benz, W., "ESA CHEOPS mission: development status," Proc. SPIE 9904, (2016).

[4] Cessa, V., Beck, T., Benz, W., Broeg, C., Ehrenreich, D., Fortier, A., Peter, G., Magrin, D., Pagano, I., Plesseria, J.-Y., Steller, M., Szoke, J., Thomas, N., Ragazzoni, R., Wildi, F., "CHEOPS: a space telescope for ultra-high precision photometry of exoplanet transits," Proc. SPIE 10563, (2017).

[5] Beck, T., Gambicorti, L., Broeg, C., Cessa, V., Fortier, A., Piazza, D., Ehrenreich, D., Magrin, D., Plesseria, J. Y., Peter, G., Pagano, I., Steller, M., Kovacs, Z., Ragazzoni, R., Wildi, F., Benz, W., "The CHEOPS (characterising exoplanet satellite) mission: telescope optical design, development status and main technical and programmatic challenges," Proc. SPIE 10562, (2017).

[6] Magrin, D., Farinato, J., Umbriaco, G., Kumar Radhakrishnan Santhakumari, K., Bergomi, M., Dima, M., Greggio, D., Marafatto, L., Ragazzoni, R., Viotto, V., Munari, M., Pagano, I., Scandariato, G., Scuderi, S., Piotto, G., Beck, T., Benz, W., Broeg, C., Cessa, V., Fortier, A., Piazza, D., "Shaping the PSF to nearly top-hat profile: CHEOPS laboratory results," Proc. SPIE 9143, (2014).

[7] Bergomi, M., Biondi, F., Marafatto, L., Dima, M., Greggio, D., Farinato, J., Magrin, D., Ragazzoni, R., Viotto, V., Gullieuszik, M., Farisato, G., Lessio, L., Portaluri, E., Munari, M., Pagano, I., Marinai, M., Novi, A., Pompei, C., Piazza, D., Beck, T., Cessa, V., Benz, W., "Aligning the demonstration model of CHEOPS," Proc. SPIE 9904, (2016).